Polymer Journal (2015) 47, 701–708

www.nature.com/pj

ORIGINAL ARTICLE

Sulfonated poly(imide-siloxane) membrane as a low vanadium ion permeable separator for a vanadium redox flow battery

Shuai Zhang, Jinchao Li, Xiaodong Huang, Yaping Zhang and Yongde Zhang

A sulfonated poly(imide-siloxane) (SPI-PDMS) membrane was prepared and evaluated for its performance in a vanadium redox flow battery (VRFB). Fourier transform infrared spectroscopy analysis verified the successful synthesis of SPI-PDMS, and scanning electron microscopy images and energy-dispersive spectroscopy results illustrated the homogeneity of the membrane. The chemical stability of the SPI-PDMS membrane was superior to that of the pristine sulfonated polyimide membrane. The as-prepared SPI-PDMS membrane showed an order-of-magnitude lower permeability of VO^{2+} ion (1.92×10^{-7} cm^2 min^{-1}) in contrast to Nafion 117 (17.1×10^{-7} cm^2 min^{-1}) and it possessed a much longer self-discharge time (550 h above 1.3 V) than Nafion 117 (65 h above 1.3 V). The SPI-PDMS-containing VRFB exhibited higher coulombic efficiency (98.50%–99.10%) at current densities ranging from 20 to 80 mA cm^{-2} than that of Nafion 117 (80.6%–94.8%). At current densities lower than 70 mA cm^{-2}, the energy efficiency of the SPI-PDMS-containing VRFB was higher than that of Nafion 117. Cyclic charge–discharge testing demonstrated that the VRFB containing the SPI-PDMS membrane had good operational stability. Overall, this low-cost SPI-PDMS membrane exhibits excellent battery performance and has considerable potential for applications in VRFBs.
Polymer Journal (2015) **47,** 701–708; doi:10.1038/pj.2015.51; published online 15 July 2015

INTRODUCTION

The vanadium redox flow battery (VRFB) has been attracting increasing attention as a promising candidate for large-scale energy storage systems because of its advantageous features, including long life, high reliability, non-pollution, low cost and high efficiency.[1–3] The proton-conductive membrane is an important component of VRFBs. The membrane must separate the catholyte and the anolyte, while allowing the passage of protons to form a circuit. The ideal proton-conductive membrane should have a low permeability to vanadium ions, high proton conductivity, good chemical stability, strong mechanical integrity and low cost.[4] To date, the perfluorinated sulfonic acid membranes such as Nafion membranes (Dupont Co., Wilmington, DE, USA) have been widely used in VRFB systems, owing to their high proton conductivity and excellent chemical stability. However, Nafion membranes also possess disadvantages such as high vanadium ion permeability and cost, which limit their large-scale commercial application in VRFB systems.[5] Consequently, a series of novel proton-conductive membranes with lower vanadium ion permeability and cost have been developed for VRFB applications such as sulfonated poly(phenylsulfone),[6] sulfonated poly(ether ether ketone)[7] and sulfonated polysulfone[8] membranes.

Sulfonated polyimide (SPI) is one of the most promising potential candidates for VRFB membranes, because the polyimide can form a compact microstructure to control vanadium ion permeability, and the introduction of sulfonic acid groups into the polymer chain makes SPI hydrophilic and facilitates the conduction of protons.[9,10] Furthermore, SPI is sufficiently thermally stable to be used in VRFBs. In our earlier work, a series of proton-conductive membranes based on SPI for VRFB applications were developed[11] and as-prepared SPI membranes showed high proton selectivity, low vanadium ion permeability and good single VRFB performance. However, pristine SPI membranes also exhibit lower antioxidant ability compared with Nafion membranes. The chemical stability of SPI membranes can be improved by adding inorganic components such as ZrO_2, AlOOH and TiO_2 through blending, to prepare composite SPI/ZrO_2,[12] SPI/AlOOH[13] and SPI/TiO_2 (Li *et al.*[14]) membranes, respectively, where the SPI and inorganic components interact with each other mainly by van der Waals forces or hydrogen bonding.

In this work, we prepared a novel sulfonated poly(imide-siloxane) (SPI-PDMS) membrane by introducing a non-sulfonated diamine segment (polydimethylsiloxane, PDMS) for VRFB applications. PDMS contains Si-O-Si main chain and methyl side groups, and therefore possesses high chemical stability, thermal stability and flexibility,[15] which is advantageous for increasing the chemical stability of as-prepared SPI-PDMS membranes. Moreover, the siloxane segment is integrated with the polyimide through strong covalent bonds. Thus, the membrane would be expected to maintain its integrity during long-term VRFB operation. The SPI-PDMS membrane was analyzed

Engineering Research Center of Biomass Materials, Ministry of Education, Southwest University of Science and Technology, Mianyang, P.R. China
Correspondence: Professor Y Zhang, Engineering Research Center of Biomass Materials, Ministry of Education, Southwest University of Science and Technology, 59, Qinglong Road, Fucheng District, Mianyang, Sichuan 621010, P.R. China.
E-mail: zhangyaping@swust.edu.cn
Received 17 March 2015; revised 20 May 2015; accepted 24 May 2015; published online 15 July 2015

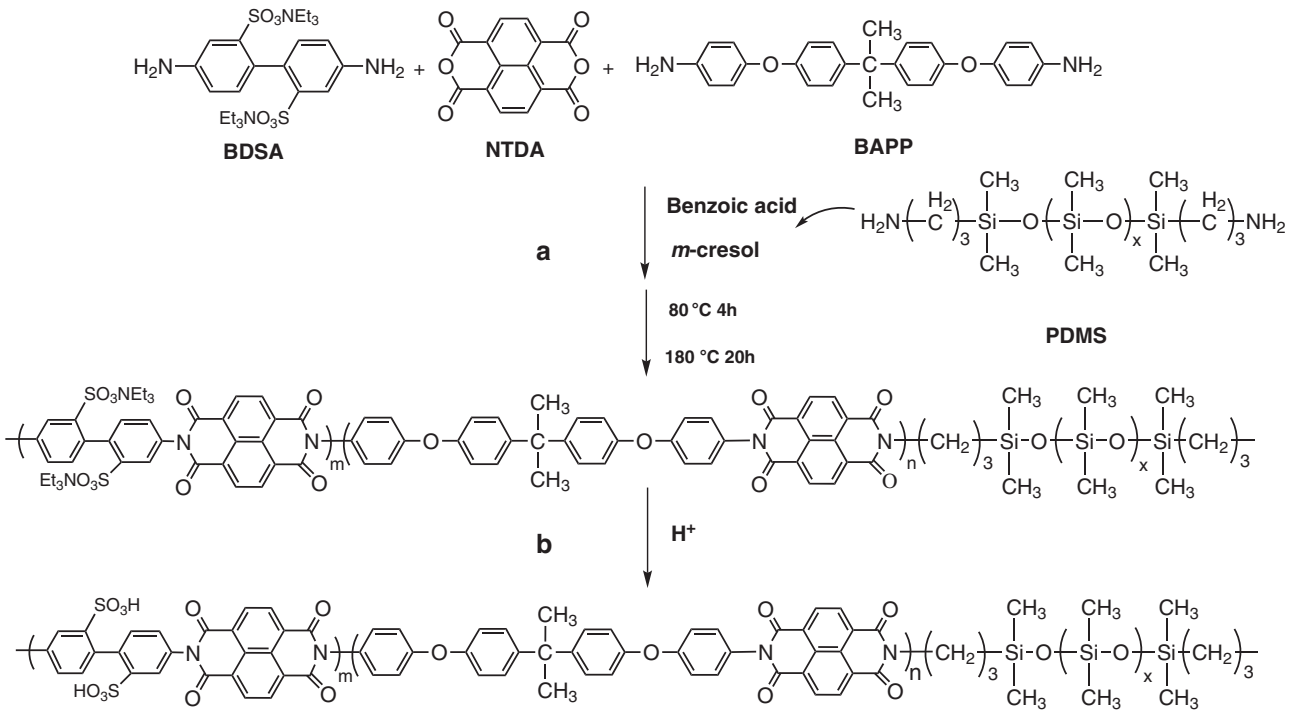

Scheme 1 Synthesis of sulfonated poly(imide-siloxane) copolymers: (**a**) synthesis of the triethylamine (TEA)-type sulfonated poly(imide-siloxane) and (**b**) protonation of the TEA-type sulfonated poly(imide-siloxane).

by Fourier transform infrared spectroscopy and scanning electron microscopy (SEM)–energy-dispersive spectroscopy. The molecular weight and molecular weight distribution of PDMS, SPI and SPI-PDMS were measured by gel-permeation chromatography. The primary properties of the membranes such as mechanical properties, chemical stability, ion-exchange capacity (IEC), proton conductivity and vanadium ion permeability were also measured. Finally, the SPI-PDMS membrane was assembled in a single VRFB and the battery performance was evaluated and discussed to preliminarily estimate its durability. To compare the VRFB performance between SPI and SPI-PDMS membranes, the charge–discharge curves at different current densities for SPI membranes were also measured.

EXPERIMENTAL PROCEDURE

Materials

The NTDA (1,4,5,8-naphthalenetetra-carboxylic dianhydride) was purchased from Beijing Multi. Tech., Beijing, China. The BDSA (4,4'-diamino-biphenyl-2,2'-disulfonic acid) was purchased from Hubei Chushengwei Chem. Co., Wuhan, China. The BAPP (4,4'-(4,4'-isopropylidenediphenyl-1,1'-diyldioxy) dianiline) was purchased from Aladdin Chem. Co., Shanghai, China. The PDMS (α,ω-diaminopropyl polydimethylsiloxane, number average molecular weight: 853 g mol^{-1}; weight average molecular weight: 959 g mol^{-1}; polydispersity index: 1.124) was purchased from Guangzhou Runpusen Chem. Co., Guangzhou, China. Vanadyl sulfate ($VOSO_4{\cdot}nH_2O$) was purchased from Shanghai Huating Chem. Plant, Shanghai, China. *m*-cresol was obtained from Shanghai Kefeng Chem. Co., Shanghai, China. Triethylamine and other reagents were obtained from Chengdu Kelong Chem. Reagent Co., Chengdu, China. Nafion 117 membrane was supplied by DuPont Co.

Preparation of the SPI-PDMS membrane

First, the SPI-PDMS was synthesized according to previously reported methods.[8] BDSA (2.80 g, 8.0 mmol), *m*-cresol (110 ml) and triethylamine (5.2 ml) were added to a three-necked round bottom flask and stirred vigorously at room temperature until the BDSA was dissolved completely. Next, 4.32 g (16 mmol) of NTDA, 2.98 g (7.26 mmol) of BAPP and 0.54 g (0.56 mmol) of PDMS were added. In addition, 3.92 g of benzoic acid were added as the catalyst. The mixture was stirred at 80 °C for 4 h, followed by heating at 180 °C for 20 h. After cooling to 80 °C, 5.0 ml of *m*-cresol were added to the solution. Then, the mixed solution was poured into 200 ml of acetone with continuous stirring applied. Acetone was used to clean the product twice, followed by drying at 80 °C for 24 h; thus, SPI-PDMS was obtained. Second, the fiber-like precipitate was dissolved into *m*-cresol forming a 7.0% (*w/v*) of SPI-PDMS solution, which was stirred vigorously. Finally, the aforementioned solution was cast onto a clean and dry glass plate and heated at 60 °C for 24 h to evaporate the solvent. The dry triethylamine-type SPI-PDMS membrane was immersed into 1.0 mol l^{-1} H_2SO_4 at room temperature for 24 h to complete the protonization process. Then, the hydrogen-type SPI-PDMS membrane was put into deionized water for 24 h to wash out residual H_2SO_4 and organic solvents completely before subsequent measurements, during which the deionized water was changed three times. The synthesis of SPI-PDMS is presented in Scheme 1.

Characterization of the membrane

Fourier transform infrared spectroscopy spectra of the membrane (4000–650 cm^{-1}, resolution 4 cm^{-1}) were measured using a Nicolet-5700 spectrometer (Thermo Nicolet Co., Madison, WI, USA).

SEM–energy-dispersive spectroscopy (Ultra 55, Zeiss Instrument Co., Berlin, Germany) was performed to analyze both the morphology and the elemental composition at the membrane surface. The measurement process was as follows: first, the SPI-PDMS membrane sample (1 cm × 1 cm) was washed in deionized water several times, then the sample was dried at 60 °C for 5 h. Second, the surface of membrane was sprayed with gold for 15 min in vacuum. Then, the surface images of the membrane sample were obtained at both ×2000 and ×5000 magnification by SEM (Ultra 55, Zeiss Instrument Co.). Concurrently, the elements on the membrane surface were measured by energy-dispersive spectroscopy.

The intrinsic viscosities of SPI and SPI-PDMS samples in *m*-cresol at 25 °C were determined using an Ubbelohde viscometer (Shanghai Shenyi Glass

Products Co., Ltd, Shanghai, China). The relative viscosity (η_r) was calculated using equation (1), the specific viscosity (η_{sp}) was calculated using equation (2) and the intrinsic viscosity ([η], dl g^{-1}) was calculated using equation (3):

$$\eta_r = \frac{\eta}{\eta_0} = \frac{t\rho}{t_0\rho_0} \approx \frac{t}{t_0} \quad (1)$$

$$\eta_{sp} = \frac{t - t_0}{t_0} \quad (2)$$

$$[\eta] = \lim_{c\to 0}\frac{\ln\eta_r}{c} = \lim_{c\to 0}\frac{\eta_{sp}}{c} \quad (3)$$

where t and t_0 are the elution time of the solvent (*m*-cresol herein) and the polymer solution, respectively, and ρ and ρ_0 are the density of the solvent and the polymer solution, respectively. When the solution is very dilute, $\rho \approx \rho_0$; c is the concentration (g ml^{-1}) of the polymer solution.

The molecular weight and molecular weight distribution of the synthesized polymers and as-purchased polymers were measured using gel permeation chromatography (Dawn Heleos II, Wyatt Tech. Co., Santa Barbara, CA, USA).

The chemical stability of the membranes was measured by soaking a membrane sample in a 0.1 mol l^{-1} VO_2^++3.0 mol l^{-1} H_2SO_4 solution at ambient temperature (25 °C). The concentration of reduced V(IV) as a function of time was measured using an ultraviolet and visible spectrophotometer (UV-1100, Shanghai Mapada Co., Shanghai, China).

The mechanical properties of the membranes were evaluated using an electronic universal testing machine (QJ-210A, Shanghai Instrument Co., Ltd, Shanghai, China) under a tensile speed of 10 mm min^{-1} at ambient temperature. The samples were cut into dumbbell shapes with a width of 4 mm in the narrow region, where the thickness of the membranes were recorded before testing.

The theoretical IEC was calculated according to the literature.[16] The experimental IEC value of the membrane was measured by titration. Protonated membranes were first immersed into a 1.0 mol l^{-1} NaCl solution for 24 h, to exchange all fixed H^+ ions of the membrane into the NaCl solution. Next, the H^+ concentration in the solution was determined by titration with a 0.04 mol l^{-1} NaOH solution and the IEC was calculated using equation (4):

$$\mathrm{IEC} = \frac{C_{\mathrm{NaOH}}\cdot V_{\mathrm{NaOH}}}{W_{\mathrm{dry}}} \quad (4)$$

where C_{NaOH} and V_{NaOH} are the concentration (mol l^{-1}) and volume (ml) of consumed NaOH solution, respectively. W_{dry} is the weight (g) of dry membrane.

The proton conductivity was determined using a four-point-probe electrochemical impedance spectroscopy at room temperature (25 °C).[17] The membrane, which measured 1.0 cm wide by 4.0 cm long, was immersed in deionized water for 24 h before testing. The testing was completed with an electrochemical workstation (CHI760C, Shanghai Chenhua Instrument Co. Ltd, Shanghai, China) in galvanostatic mode with 5.0 mA of current over a frequency range of 1.0 Hz to 100 kHz. The electric resistance was measured in a Teflon cell consisting of two stainless steel flat outer current-carrying electrodes and two platinum wire inner potential-sensing electrodes. The proton conductivity was calculated using equation (5):

$$\sigma = \frac{L}{R\cdot d\cdot w} \quad (5)$$

where σ is the proton conductivity (S cm^{-1}), R is the membrane resistance (Ω), and d and w are the thickness (cm) and width (cm) of the membrane, respectively. L is the distance (cm) between the two platinum wires.

The VO^{2+} permeability measurement was conducted in a membrane-separated cell using the standard procedure as reported in the literature at 25 °C.[12] The VO^{2+} permeability was determined using equation (6):

$$V\frac{\mathrm{d}Ct}{\mathrm{d}t} = A\frac{P}{d}(C_0 - C_t) \quad (6)$$

where V is the solution volume (cm^3) in each half-cell, A is effective membrane area (cm^2), P is the permeability parameter (cm^2 min^{-1}) of vanadium ions, C_0 is the initial concentration (mol l^{-1}) of vanadium ions and C_t is the crossed vanadium ion concentration (mol l^{-1}) at time t (min) in the right half-cell.

Table 1 The M_w, M_n, PDI and [η] of the polymers studied

Membrane	M_w[a] (g mol^{-1})	M_n (g mol^{-1})	*PDI*[b]	[η][c]
SPI	144 890	138 080	1.049	0.82
SPI-PDMS	158 230	153 090	1.034	1.09
PDMS	959	853	1.124	—

Abbreviations: [η], intrinsic viscosity; M_n, number average molecular weight; M_w, weight average molecular weight; PDI, polydispersity index; PDMS, polydimethylsiloxane; SPI, sulfonated polyimide; SPI-PDMS, sulfonated poly(imide-siloxane).
[a]Determined using laser (LS) detection.
[b]PDI = M_w/M_n.
[c]Measured at 25 °C.

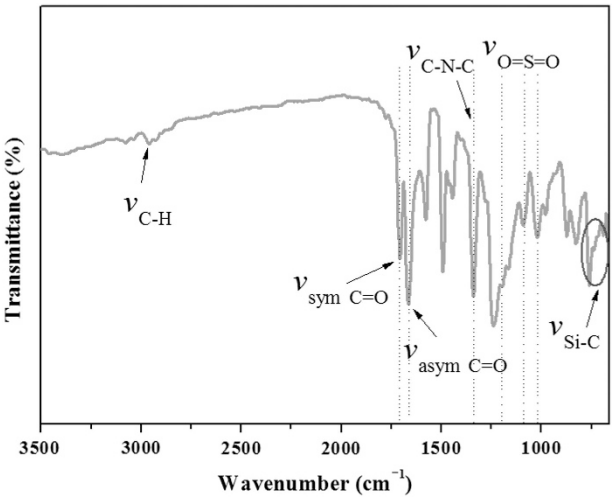

Figure 1 Fourier transform infrared spectroscopy (FT-IR) spectra of the SPI-PDMS membrane. A full color version of this figure is available at *Polymer Journal* online.

A single VRFB was fabricated by sandwiching the membrane between two pieces of carbon-felt electrodes,[14] with an effective area and thickness of 8.0 cm^2 and 10 mm, respectively. A graphite plate was used as the current collector. Thirty milliliters of 1.5 mol l^{-1} VO^{2+} in 3.0 mol l^{-1} H_2SO_4 solution and 30 ml of 1.5 mol l^{-1} V^{3+} in 3.0 mol l^{-1} H_2SO_4 solution were used as the positive and the negative electrolytes, respectively. The fabricated single battery was charged–discharged using a battery testing system (CT-3008-5V/3A-S1, Xinwei Neware, Shenzhen, China) with a constant current density ranging from 20 to 80 mA cm^{-2}. The upper limit of charge voltage and lower limit of discharge voltage were 1.65 and 0.8 V, respectively. The coulombic efficiency (CE), energy efficiency (EE) and voltage efficiency (VE) of the VRFB are calculated using equations (7,8,9).

$$\mathrm{CE}(\%) = \frac{\text{discharge capacity (mA } h)}{\text{charge capacity (mA } h)} \times 100 \quad (7)$$

$$\mathrm{EE}(\%) = \frac{\text{discharge energy (mW } h)}{\text{charge energy (mW } h)} \times 100 \quad (8)$$

$$\mathrm{VE}(\%) = \frac{\mathrm{EE}}{\mathrm{CE}} \times 100 \quad (9)$$

RESULTS AND DISCUSSION

Viscosity and molecular weight of SPI-PDMS

The intrinsic viscosity of SPI-PDMS and pristine SPI are 1.09 and 0.82 dl g^{-1}, respectively (Table 1). Moreover, both the weight average molecular weight and the number average molecular weight of SPI-PDMS are measured to be 158 230 g mol^{-1} and 153 090 g mol^{-1},

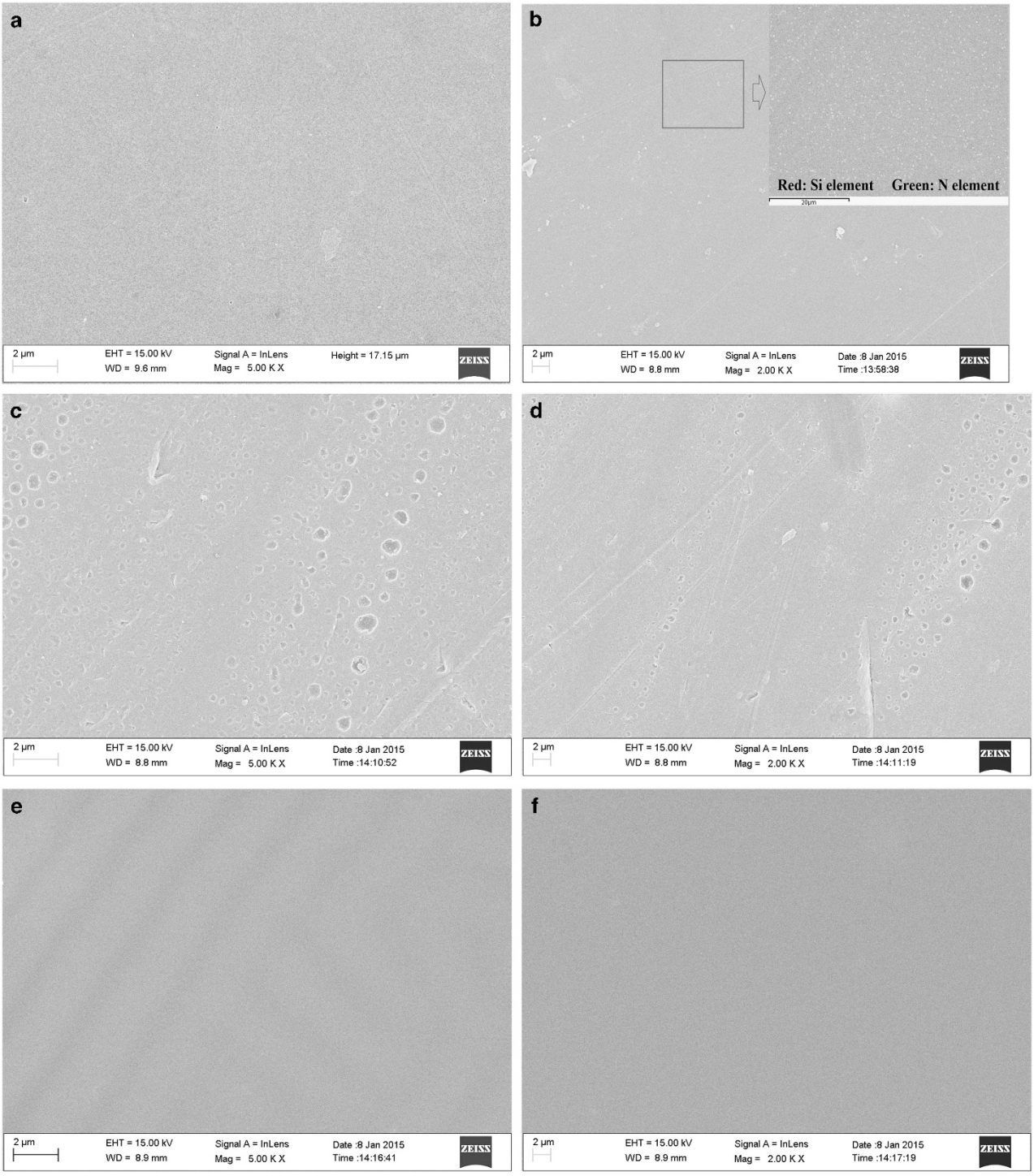

Figure 2 SEM images of SPI-PDMS membrane at both ×2000 and ×5000 magnifications. (**a** and **b**) Initial surfaces (inserted image in **b** is the energy-dispersive spectroscopy (EDS) of membrane surface). (**c** and **d**) Surfaces after VRFB cycling test (facing the anode). (**e** and **f**) Surfaces after VRFB cycling test (facing the cathode). A full color version of this figure is available at *Polymer Journal* online.

respectively, which are both larger than those of pristine SPI. These results verify that polymeric products were obtained.

Membrane structure and morphology

The chemical structure of the as-prepared SPI-PDMS membrane was confirmed by Fourier transform infrared spectroscopy (Figure 1). The characteristic absorption bands of the imide carbonyl groups (C = O) are observed at ~ 1711 (symmetric) and 1667 cm^{-1} (asymmetric), and the C–N–C stretching vibration of the imide ring is observed at ~ 1344 cm^{-1}. The absorptions at 1025, 1095 and 1201 cm^{-1}, which are related to the stretch vibration of sulfonic acid group (O = S = O), are also observed. The C–H stretch of the methyl group associated with BAPP and PDMS is observed at 2962 cm^{-1}. However, this signal overlaps with the absorption resulting from the sulfonic acid group,

which is in the same region. The band at 704–760 cm^{-1} is due to the Si–C stretch.[18,19] These results verify the successful synthesis of SPI-PDMS.

The morphology of the SPI-PDMS membrane was examined using SEM and the surface images of the membrane before and after performing 100 VRFB cycling tests are shown in Figures 2a–f. As shown in Figures 2a and b, the initial SPI-PDMS membrane is homogeneous and no pores or cracks in the membrane are observable at different magnification levels. The surface image of SPI-PDMS membrane (facing the anode) after a VRFB cycling test is presented in Figures 2c and d. As evidenced by the images, the membrane surface facing the anode is covered with small concave features compared with the pristine SPI-PDMS membrane. This result implies that slight corrosion occurs after the membrane is in contact with a strong oxidative (VO_2^+/VO^{2+}) solution for some time. The SEM image of the surface of SPI-PDMS membrane (facing the cathode) after the same VRFB cycling test is shown in Figures 2e and f. There is little change at the membrane surface compared with its untested surface, verifying the chemical stability of SPI-PDMS membrane at the cathode side. As the same concentration of H_2SO_4 (3.0 mol l^{-1}) exists in both the catholyte and the anolyte, the difference in SEM images of both sides of the SPI-PDMS membrane is mainly a result of the valence of vanadium ions in the catholyte and the anolyte. Obviously, the oxidative ability of the anolyte is stronger than that of catholyte; thus, the SPI-PDMS membrane facing the anode is oxidized more significantly. Similar experimental results were also reported by Zhang *et al.*[20] The dispersion of PDMS in the SPI-PDMS membrane was also investigated by energy-dispersive spectroscopy and the result is shown in Figure 2b. The element Si (red markers), originating from PDMS, and the element N (green markers), originating from the imide ring, are both uniformly distributed at the surface of SPI-PDMS membrane, further indicating that the PDMS was successfully introduced into SPI-PDMS membrane. This result is in accordance with the conclusions deduced from the Fourier transform infrared spectroscopy spectra shown in Figure 1.

Chemical stability and mechanical properties of membranes

Chemical stability is of vital importance for commercial applications of the proton-conductive membrane in VRFBs, especially for non-fluorinated polymer membranes. In this study, the membranes were oxidized by VO_2^+ and the variation of the concentration of VO_2^+ reduced by SPI, SPI-PDMS and Nafion 117 are shown in Figure 3. Even after soaking the membranes in VO_2^+ solution for 288 h, the pristine SPI, SPI-PDMS and Nafion 117 membranes all appear to be intact, indicating that the membranes are durable in V(V) solution. Among the three membranes, the pristine SPI membrane shows the largest quantity of VO_2^+ reduced, indicating its weak anti-oxidation stability. Nafion 117 membrane is the most stable, owing to its solid C–F backbone.[21] In addition, the SPI-PDMS membrane has a better oxidation stability than the pristine SPI membrane, because the siloxane segment can improve the anti-oxidation stability of SPI-PDMS membrane. However, the as-prepared SPI-PDMS membrane still demonstrates a weaker chemical stability than either Nafion 117 as most non-fluorinated polymer membranes such as sulfonated poly(ether ether ketone)[22] and sulfonated dielsalder poly

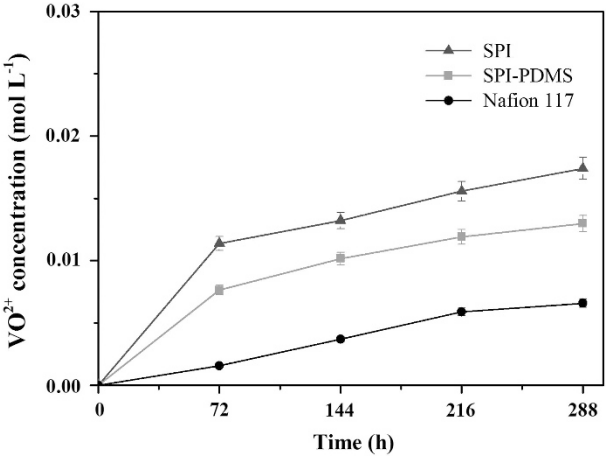

Figure 3 Variation of the concentration of VO^{2+} reduced by the pristine SPI, SPI-PDMS and Nafion 117 membranes with time. A full color version of this figure is available at *Polymer Journal* online.

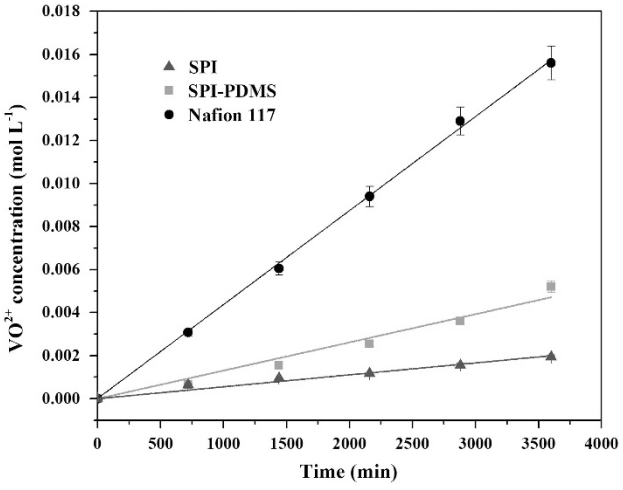

Figure 4 Concentration changes of VO^{2+} ion across SPI, SPI-PDMS and Nafion 117 membranes with time. A full color version of this figure is available at *Polymer Journal* online.

Table 2 Physicochemical properties of SPI, SPI-PDMS and Nafion 117 membranes

		IEC (meq g^{-1})						
Membrane	*Thickness (μm)*	*Theoretical*[b]	*Experimental*	*Proton conductivity* ($\times10^{-2}$ S cm^{-1})	*VO^{2+} permeability* ($\times10^{-7}$ cm^2 min^{-1})	*Proton selectivity* ($\times10^5$ S min cm^{-3})	*S (MPa)*[a]	*E (%)*
SPI	62 ± 3	1.56	1.49	3.17	0.48	6.60	55.23	12.69
SPI-PDMS	57 ± 3	1.35	1.33	3.26	1.92	1.70	47.16	17.81
Nafion 117	175 ± 3	—	1.13	5.82	17.10	0.34	23.18	156.0

Abbreviations: *E*, elongation at break; IEC, ion-exchange capacity; *S*, stress at break; SPI, sulfonated polyimide; SPI-PDMS, sulfonated poly(imide-siloxane).
[a]Measured in dry membrane.
[b]The theoretical IEC can be calculated according to literature.[16]

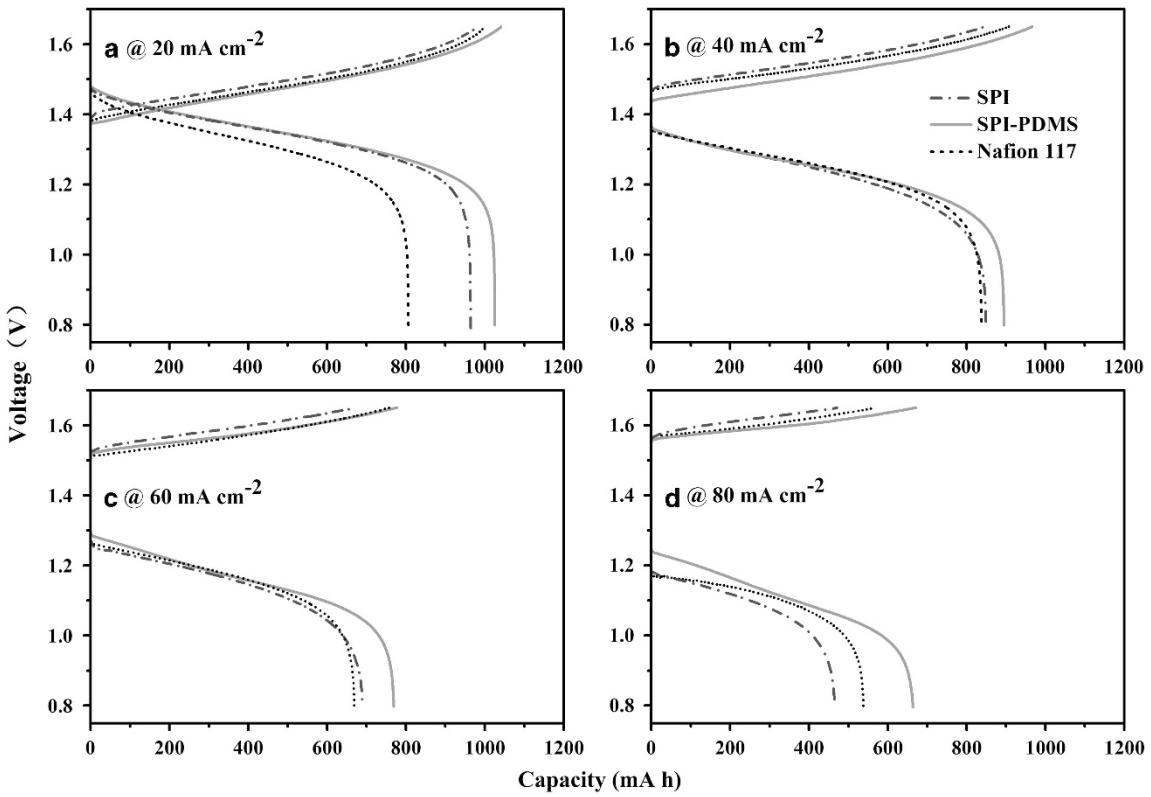

Figure 5 Charge–discharge curves for VRFBs with SPI, SPI-PDMS and Nafion 117 membranes at the current density of (**a**) 20, (**b**) 40, (**c**) 60 and (**d**) 80 mA cm^{-2}. A full color version of this figure is available at *Polymer Journal* online.

(phenylene)s.[6] As a result, more studies should be carried out to overcome this disadvantage.

Next, the mechanical properties of membranes were characterized by maximum stress at break (*S*) and elongation at break (*E*), and the data are presented in Table 2. The SPI-PDMS membrane has a much higher maximum stress at break than Nafion 117, which is attributed to the robust aromatic backbone. However, the elongation at break of SPI-PDMS membranes is markedly decreased when compared with that of Nafion 117 membranes. This is possibly because the Nafion 117 membrane contains flexible aliphatic main chains.

IEC, vanadium ion permeability, proton conductivity and proton selectivity of the membrane

The theoretical IEC (1.35 mmol g^{-1} dry) and measured IEC (1.33 mmol g^{-1} dry) of as-prepared SPI-PDMS membranes are similar, as shown in Table 2. A good proton-conductive membrane in a VRFB should possess low vanadium ion permeability. Figure 4 shows the change of crossed VO^{2+} concentration with time under identical conditions for all membranes. The crossed VO^{2+} concentration of the SPI-PDMS membrane increases with time slightly faster than that of the pristine SPI membrane. However, it increases much more slowly than that of the Nafion 117 membrane. The VO^{2+} permeability coefficients of the pristine SPI, SPI-PDMS and Nafion 117 membranes are calculated to be 0.48×10^{-7}, 1.92×10^{-7} and 17.10×10^{-7} cm^2 min^{-1}, respectively. The VO^{2+} permeability coefficient difference between SPI, SPI-PDMS and Nafion 117 membranes can be explained by their microstructures. Water and ions move through the interconnected hydrated ionic channel structures of sulfonated polymer membranes.[23] The pristine SPI and SPI-PDMS membranes have less hydrophobic/hydrophilic phase separation than Nafion and the VO^{2+} transport channels are more narrow and branched in SPI and SPI-PDMS membranes compared with those in Nafion, leading to lower permeability of vanadium ions.[24] Moreover, the siloxane segment of the SPI-PDMS membrane possibly affects the compactness of the membrane microstructure; therefore, the VO^{2+} permeability coefficient of SPI-PDMS is larger than that of the pristine SPI. Nevertheless, the SPI-PDMS membrane is still a promising candidate to inhibit vanadium ion cross-over in VRFBs, especially considering its much lower vanadium ion permeability in comparison with Nafion 117 membranes.

The proton conductivity for the pristine SPI, SPI-PDMS and Nafion 117 membranes at room temperature were measured and the results are shown in Table 2. The SPI-PDMS membranes with flexible non-sulfonated diamine-PDMS moieties tend to have satisfactory proton conductivity, because their flexibility readily allows for the relaxation of the polymer chains.[25] The SPI-PDMS membrane incorporating PDMS at 5.0 wt% typically exhibits a close proton conductivity (3.26×10^{-2} S cm^{-1}) to that of pristine SPI with no PDMS segments (3.17×10^{-2} S cm^{-1}). However, the proton conductivity of SPI-PDMS membrane is still a little lower than that of Nafion 117 (5.82×10^{-2} S cm^{-1}), because the unique hydrophilic–hydrophobic structure of Nafion membrane is essential to its proton conductivity.

The proton conductivity and vanadium ion permeability are usually found to have an antagonistic relationship.[26] Therefore, the proton selectivity, defined as the ratio of proton conductivity to vanadium ion permeability, is currently applied to evaluate the comprehensive performance of membranes. The proton conductivity, vanadium ion permeability and proton selectivity of the pristine SPI, SPI-PDMS and Nafion 117 membranes are shown in Table 2. The proton selectivity of SPI-PDMS membrane (1.70×10^5 S min cm^{-3}) is markedly higher

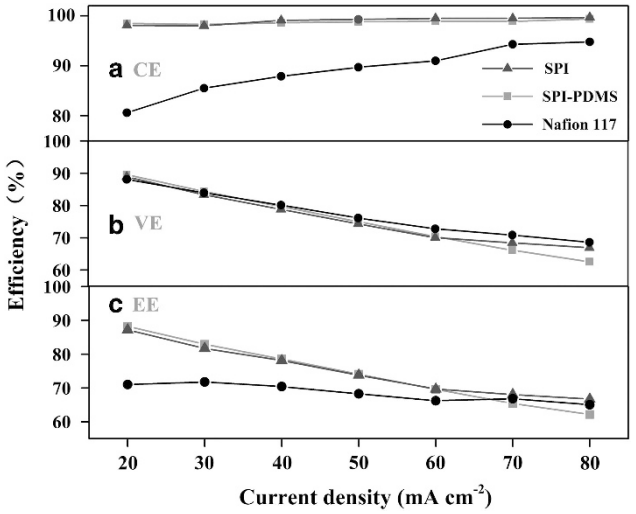

Figure 6 Variation of (**a**) coulombic efficiency (CE), (**b**) voltage efficiency (VE) and (**c**) energy efficiency (EE) of VRFBs with SPI, SPI-PDMS and Nafion 117 membranes at different current density. A full color version of this figure is available at *Polymer Journal* online.

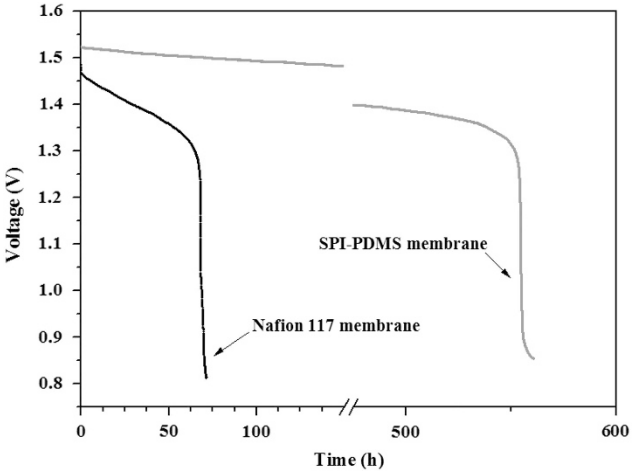

Figure 7 Open-circuit voltage (OCV) of VRFBs with SPI-PDMS and Nafion 117 membranes. A full color version of this figure is available at *Polymer Journal* online.

than that of Nafion 117 (0.34×10^5 S min cm^{-3}), but lower than that of the pristine SPI (6.60×10^5 S min cm^{-3}), which is mainly due to the vanadium ion permeability difference between SPI, SPI-PDMS and Nafion 117.

Single VRFB performance

The charge–discharge curves of a VRFB containing SPI, SPI-PDMS or Nafion 117 membranes at different current densities are illustrated in Figure 5. As shown, the discharge capacity of a VRFB with SPI-PDMS is higher than a VRFB with Nafion 117 at all charge–discharge current densities because of its lower vanadium ion permeability. The higher utilization rate of electrolytes for SPI-PDMS membranes leads to the increase of battery capacity.[27] However, the discharge capacity of SPI is similar to that of Nafion 117 at 40 and 60 mA cm^{-2}, whereas it is lower than that of Nafion 117 at 80 mA cm^{-2}, even though the vanadium ion permeability of SPI is much lower than that of Nafion 117. This is primarily because the chemical stability of SPI is much

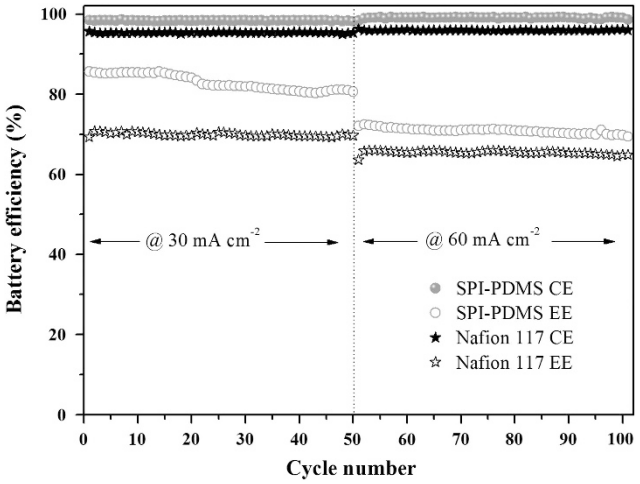

Figure 8 Cycle performances of VRFBs with SPI-PDMS and Nafion 117 membranes at current densities of 30 (50 cycles) and 60 mA cm^{-2} (50 cycles), respectively. A full color version of this figure is available at *Polymer Journal* online.

weaker than that of Nafion 117. When the current density is as high as 80 mA cm^{-2}, this chemical instability of SPI is particularly disadvantageous to its discharge capacity. Therefore, decreasing the vanadium ion permeability and increasing the chemical stability are both very important for maintaining the battery capacity for VRFB membranes. Furthermore, a relatively high discharge voltage of a VRFB with SPI-PDMS is obtained over the entire charge–discharge current range due to the low permeation of vanadium ions. With the increase of current density, charge–discharge capacity decreases overall due to the stronger polarization effect at high current density.[28]

The variations of CE/VE/EE as a function of current density are shown in Figure 6. The CE of a SPI-PDMS membrane is slightly lower than that of a pristine SPI membrane because of its higher vanadium ion permeability. As our single VRFB is of laboratory scale, the CE for SPI and SPI-PDMS are both very high and the difference between the CE of SPI and SPI-PDMS membranes is small. However, the CE of a VRFB with an SPI-PDMS membrane achieves above 98% at all current densities, which is higher than that of Nafion 117; this is especially interesting at low current density, considering that the vanadium ion permeability of SPI-PDMS is lower than that of Nafion 117. The CE of the VRFB with a Nafion membrane increases with rising current density, because the charge–discharge reactions proceed faster at a higher current density and the side reactions and vanadium cross-over are suppressed. The VE for all membranes decreases with increasing current density because of the high overpotential and ohmic potential drop at high current density.[29] In general, the VE for the SPI and SPI-PDMS is similar to that of Nafion 117 but slightly lower than Nafion 117 at high current density. This is because the proton conductivity of SPI and SPI-PDMS is slightly lower than that of Nafion 117, as presented in Table 2. As a comprehensive estimation standard for practical batteries, the EE is used to compare the battery performance of the as-prepared SPI and SPI-PDMS membranes and commercial Nafion 117. As indicated in Figure 6, the VRFB-containing SPI or SPI-PDMS exhibits higher EE at 20–60 mA cm^{-2}, suggesting that the application of both membranes can significantly increase the VRFB performance, especially at low current density. This result further validates the outstanding proton selectivity of the SPI and SPI-PDMS as presented in 'IEC, vanadium ion permeability, proton conductivity and proton selectivity of the membrane'.

Although the proton selectivity of an SPI-PDMS membrane is slightly lower than that of an SPI membrane, the chemical stability of SPI-PDMS is better than SPI. The single VRFB performance of an SPI-PDMS membrane is very close to that of a pristine SPI membrane, confirming that as-prepared SPI-PDMS membranes are potential candidates for VRFB applications.

In addition, we also studied the self-discharge behavior of the VRFBs with as-prepared SPI-PDMS membrane and commercial Nafion 117 by monitoring their open-circuit voltage over time (see Figure 7). Surprisingly, the VRFB assembled with the SPI-PDMS membrane maintains an open-circuit voltage above 1.3 V for ~ 550 h, which is ~ 8.5 times longer than that for the VRFB with Nafion 117 (~65 h). This result confirms that the SPI-PDMS membrane functions considerably better than Nafion 117 at a suppressing vanadium cross-over in the VRFB.

The stability of the as-prepared SPI-PDMS membrane in a VRFB was also measured by carrying out 50 charge–discharge cycles at the current density of 30 mA cm^{-2} and another 50 cycles at 60 mA cm^{-2}, the results of which are shown in Figure 8. When the current density is 30 mA cm^{-2}, the VRFB with an SPI-PDMS membrane maintains CE beyond 98% and EE ~ 81% during 50 cycles. When the current density is elevated to 60 mA cm^{-2} for the second set of 50 cycles, the CE and EE are 9%9 and 72%, respectively. Both CE and EE values of the VRFB with an as-prepared SPI-PDMS membrane exceed those with Nafion 117. These results demonstrate that SPI-PDMS exhibits high stability and excellent VRFB performance, and it is a potential substitute for the currently used Nafion 117 for VRFB applications.

CONCLUSIONS

We successfully prepared an SPI-PDMS membrane that exhibits significantly lower vanadium ion permeability and lower cost than commercial Nafion 117. The SPI-PDMS membrane's self-discharge rate is sharply reduced. Both CE and energy efficiency of the VRFB are improved by using SPI-PDMS membranes instead of Nafion 117 over a current density range of 20–60 mA cm^{-2}. Cycling charge–discharge tests demonstrated the good operational stability of the as-prepared SPI-PDMS membrane. Considering its excellent battery performance and reasonable cost, the SPI-PDMS membrane shows a promising application prospect in VRFBs.

ACKNOWLEDGEMENTS

Financial supports from the National Natural Scientific Foundation of China (number 21206138), the Key Fund Project of Sichuan Provincial Department of Education (number 12ZA181) and the Postgraduates Innovation Fund of Southwest University of Science and Technology (number 14ycx004) are greatly appreciated.

1 Skyllas-Kazacos, M., Robins, R. G. & Fane, A. G. New all vanadium redox flow cell. *J. Electrochem. Soc.* **133**, 1057–1058 (1986).
2 Álvaro, C., Nuno, R. & Brito, F. P. Vanadium redox flow batteries: a technology review. *Int. J. Energy Res.* **39**, 889–918 (2014).
3 Alotto, P., Guarnieri, M. & Moro, F. Redox flow batteries for the storage of renewable energy: a review. *Renew. Sust. Energ. Rev.* **29**, 325–335 (2014).
4 Li, X., Zhang, H., Mai, Z., Zhang, H. & Vankelecom, I. Ion exchange membranes for vanadium redox flow battery (VRB) applications. *Energ. Environ. Sci.* **4**, 1147–1160 (2011).
5 Sun, C., Chen, J., Zhang, H., Han, X. & Luo, Q. Investigations on transfer of water and vanadium ions across Nafion membrane in an operating vanadium redox flow battery. *J. Power Sources* **195**, 890–897 (2010).
6 Fujimoto, C., Kim, S., Stains, R., Wei, X., Li, L. & Yang, Z. G. Vanadium redox flow battery efficiency and durability studies of sulfonated Diels Alder poly(phenylene)s. *Electrochem. Commun.* **20**, 48–51 (2012).
7 Li, Z., Xi, J., Zhou, H., Liu, L., Wu, Z., Qiu, X. & Chen, L. Preparation and characterization of sulfonated poly(ether ether ketone)/poly(vinylidene fluoride) blend membrane for vanadium redox flow battery application. *J. Power Sources* **237**, 132–140 (2013).
8 Kim, S., Yan, J., Schwenzer, B., Zhang, J., Li, L., Liu, J., Yang, Z. & Hickner, M. A. Cycling performance and efficiency of sulfonated poly(sulfone) membranes in vanadium redox flow batteries. *Electrochem. Commun.* **12**, 1650–1653 (2010).
9 Genies, C., Sillion, B., Petiaud, R., Cornet, N., Gebel, G. & Pineri, M. Stability study of sulfonated phthalic and naphthalenic polyimide structures in aqueous medium. *Polymer* **42**, 5097–5105 (2001).
10 Yamazaki, K. & Kawakami, H. High proton conductive and low gas permeable sulfonated graft copolyimide membrane. *Macromolecules* **43**, 7185–7191 (2010).
11 Zhang, Y., Li, J., Zhang, H., Zhang, S. & Huang, X. Sulfonated polyimide membranes with different non-sulfonated diamines for vanadium redox battery applications. *Electrochim. Acta* **150**, 114–122 (2014).
12 Li, J., Zhang, Y., Zhang, S., Huang, X. & Wang, L. Novel sulfonated polyimide/ZrO_2 composite membrane as a separator of vanadium redox flow battery. *Polym. Advan. Technol.* **25**, 1610–1615 (2014).
13 Zhang, Y., Li, J., Wang, L. & Zhang, S. Sulfonated polyimide/AlOOH composite membranes with decreased vanadium permeability and increased stability for vanadium redox flow battery. *J. Solid State Electrochem.* **18**, 3479–3490 (2014).
14 Li, J., Zhang, Y. & Wang, L. Preparation and characterization of sulfonated polyimide/TiO_2 composite membrane for vanadium redox flow battery. *J. Solid State Electrochem.* **18**, 729–737 (2013).
15 Tanardi, C. R., Pinheiro, A. F., Nijmeijer, A. & Winnubst, L. PDMS grafting of mesoporous γ-alumina membranes for nanofiltration of organic solvents. *J. Membr. Sci.* **469**, 471–477 (2014).
16 Liu, S., Wang, L., Zhang, B., Liu, B., Wang, J. & Song, Y. Novel sulfonated polyimide/polyvinyl alcohol blend membranes for vanadium redox flow battery applications. *J. Mater. Chem. A* **3**, 2072–2081 (2015).
17 Sone, Y., Ekdunge, P. & Daniel, S. Proton conductivily of Nafion 117 as measured by a four-electrode AC impedance method. *J. Electrochem. Soc.* **143**, 1254–1259 (1996).
18 Lee, C., Chen, J., Shiu, H., Ho, K., Wu, S., Hsieh, K. & Wang, Y. Effect of bridging groups on sulfonated poly(imide-siloxane) for application in proton exchange membrane. *J. Fuel Cell Sci. Technol.* **7**, 021023 (2010).
19 Tseng, C., Ye, Y., Joseph, J., Kao, K., Rick, J., Huang, S. & Hwang, B. Tuning transport properties by manipulating the phase segregation of tetramethyldisiloxane segments in modified polyimide electrolytes. *J. Power Sources* **196**, 3470–3478 (2011).
20 Zhang, H., Li, X., Mai, Z., Wei, W. & Li, Y. Crosslinkable sulfonated poly(diallyl-bisphenol ether ether ketone) membranes for vanadium redox flow battery application. *J. Power Sources* **217**, 309–315 (2012).
21 Liu, S., Wang, L., Ding, Y., Liu, B., Han, X. & Song, Y. Novel sulfonated poly(ether ether keton)/polyetherimide acid-base blend membranes for vanadium redox flow battery applications. *Electrochim. Acta* **24**, 90–102 (2014).
22 Li, Z., Dai, W., Yu, L., Liu, L., Xi, J., Qiu, X. & Chen, L. Properties investigation of sulfonated poly(ether ether ketone)/polyacrylonitrile acid-base blend membrane for vanadium redox flow battery application. *ACS Appl. Mater. Interfaces* **6**, 18885–18893 (2014).
23 Kreuer, K. D. On the development of proton conducting polymer membranes for hydrogen and methanol fuel cells. *J. Membr. Sci.* **185**, 29–39 (2001).
24 Qiu, J., Zhang, J., Chen, J., Peng, J., Xu, L., Zhai, M., Li, J. & Wei, G. Amphoteric ion exchange membrane synthesized by radiation-induced graft copolymerization of styrene and dimethylaminoethyl methacrylate into PVDF film for vanadium redox flow battery applications. *J. Membr. Sci.* **334**, 9–15 (2009).
25 Lee, C., Chen, S., Wang, Y., Lin, C., Huang, C., Chuang, C., Wang, C. & Hsieh, K. Preparation and characterization of proton exchange membranes based on semi-interpenetrating sulfonated poly(imide-siloxane)/epoxy polymer networks. *Energy* **55**, 905–915 (2013).
26 Chen, D., Kim, S., Li, L., Yang, G. & Hickner, M. A. Stable fluorinated sulfonated poly (arylene ether) membranes for vanadium redox flow batteries. *RSC Adv.* **2**, 8087–8094 (2012).
27 Luo, Q., Zhang, H., Chen, J., You, D., Sun, C. & Zhang, Y. Preparation and characterization of Nafion/SPEEK layered composite membrane and its application in vanadium redox flow battery. *J. Membr. Sci.* **325**, 553–558 (2008).
28 Skyllas-Kazacos, M. & Mohammadi, T. Preparation of sulfonated composite membrane for vanadium redox flow battery applications. *J. Membr. Sci.* **107**, 35–45 (1995).
29 Wei, W., Zhang, H., Li, X., Zhang, H., Li, Y. & Vankelecom, I. Hydrophobic asymmetric ultrafiltration PVDF membranes: an alternative separator for VFB with excellent stability. *Phys. Chem. Chem. Phys.* **15**, 1766–1771 (2013).